Polymer 51 (2010) 3075–3082

Contents lists available at ScienceDirect

Polymer

journal homepage: www.elsevier.com/locate/polymer

Facile preparation of curved polymer composite nanosheets

Ying Wu [a,b], Liyan Huang [a], Zhengping Liu [a,*], Zhenzhong Yang [b,**]

[a] Institute of Polymer Chemistry and Physics of College of Chemistry, BNU Key Laboratory of Environmentally Friendly and Functional Polymer Materials, Beijing Normal University, Beijing 100875, China
[b] State Key Laboratory of Polymer Physics and Chemistry, Institute of Chemistry, Chinese Academy of Sciences, Beijing 100080, China

ARTICLE INFO

Article history:
Received 17 January 2010
Received in revised form
17 April 2010
Accepted 26 April 2010
Available online 20 May 2010

Keywords:
Nanosheets
Polymer nanocomposites
Miniemulsion polymerization

ABSTRACT

A facile no-template approach for fabricating curved polystyrene (PS) nanosheets by miniemulsion polymerization technique was developed. Two essences of the high hydrophobicity of oil phase and the existence of cross-linking comonomer were found to ensure the stable curved sheet-like morphology. Here, when choosing tetradecane as the hydrophobic oil phase and divinylbenzene as cross-linker, the curved PS nanosheets with stable structure were obtained. Furthermore, after introducing functional groups by sulfonation reaction, these curved PS nanosheets can be used as a general template for preparing curved sheet-like inorganic/organic nanocomposites with broadly varied inorganic ingredients, such as metal Ag nanoparticles, inorganic titania, silica, etc. Otherwise, when calcining or carbonizing these inorganic/organic nanocomposites under air or nitrogen, novel mesoporous or microporous pure inorganic nanomaterials with curved sheet-like morphology were obtained conveniently further.

© 2010 Elsevier Ltd. All rights reserved.

1. Introduction

In the past decades, efforts in the field of nanomaterials have mainly been focused on fabricating one-dimensional nanowires, nanorods and nanotubes [1]. Comparatively, two-dimensional nanosheets have attracted increasing interests just recently, due to their unique structure of two-dimensional anisotropy [2,3] and resulted potential applications for fabricating novel functional nanomaterials [4,5].

Until now, many methods have been developed to synthesize two-dimensional inorganic or composite nanosheets, such as exfoliation of the layered precursor [6–8], thermochemical or thermophysical reaction process [9–15], liquid–liquid interfacial precipitation method [16], and so on. However, for preparing two-dimensional polymeric nanosheets, only few methods have been reported. As the first example in this field, separate polymer nanosheets containing phenanthrene, anthracene, and dinitrobenzene chromophore have been prepared by the Langmuir–Blodgett technique [17], in which the rather tedious synthesis procedure for special spreading polymer was unavoidable. Secondly, high-performance aromatic polyimide nanosheets were synthesized via a monomer adsorption and polycondensation process occurred inside the pores of mesoporous silica monoliths [18]. Similarly, unique polymer nanosheets were also formed by thermal polymerization of styrene or methyl methacrylate bicontinuous microemulsions from the gaps of a silica opal membrane [19]. Unfortunately, in the latter two techniques, it is complicated to prepare sheet-like materials in scales. As a result, it is still an urgent requirement now to develop a simple single-step, scalable strategy for preparing polymer nanosheets.

Emulsion polymerization had been proved as a powerful technique for controlling the morphologies of obtained polymer particles. By simply manipulating the polymerization conditions, novel polymer particles with various morphologies were obtained, such as inverse core-shell, double hemispherical, onion-like, golf-ball-like, peanut-like particles and hollow spheres, etc. [20–25] With the increasing requirements for nanomaterials, miniemulsion polymerization, a variant of the emulsion polymerization, in which monomer droplets play a key role in particle nucleation, has attracted extra attention in very recent years, because the polymer particles with submicrometer size, more controllable morphologies and special functionalities can be obtained, besides of the inherent virtues of the emulsion polymerization [26–35]. For example, through miniemulsion polymerization, crumpled poly(acrylonitrile) particles composed of 10 nm large polymer nanocrystals [29], organic-inorganic polystyrene-silica hybrid asymmetric particles [30], polymeric capsules encapsulated with many different kinds of materials [32–35] were all produced. Unfortunately, to the best of our knowledge, there has been no report on preparing

* Corresponding author. Fax: +86 10 58802075.
** Corresponding author. Fax: +86 10 62559373.
E-mail addresses: lzp@bnu.edu.cn (Z. Liu), yangzz@iccas.ac.cn (Z. Yang).

0032-3861/$ – see front matter © 2010 Elsevier Ltd. All rights reserved.
doi:10.1016/j.polymer.2010.04.056

nanomaterials with two-dimensional sheet-like morphology by one-step miniemulsion polymerization until now.

Herein, we demonstrated a novel one-pot non-templating synthetic method to prepare curved PS nanosheets by virtue of miniemulsion polymerization technique. Furthermore, we also showed that these novel curved PS nanosheets can be used as templates for preparing two-dimensional sheet-like nanocomposites with changeable compositions such as metals, inorganic materials, etc.

2. Experimental section

2.1. Materials

Styrene (St) and divinylbenzene (DVB) were passed through an activated Al_2O_3 column to remove the inhibitors and stored at low temperature for use. Aniline was distilled under vacuum and stored at low temperature. 2-Azoisobutyronitrile (AIBN) was recrystallized from methanol and stored at 4 °C. Tetraethyl orthosilicate (TEOS), tetrabutyl titanate (TBT), sodium dodecyl sulfate (SDS), tetradecane (TD), isooctane (OT), potassium persulfate (KPS) and ethanol were used without further purification.

2.2. Sample preparation

2.2.1. Synthesis of PS nanosheets by miniemulsion polymerization

A representative polymerization process was as follows: surfactant of SDS (0.03 g) and water (15 mL) were mixed together by ultrasonicating for a few minutes. A mixture of TD (2.1 mL), St (1.5 mL) and DVB (0.5 mL) was then added. The miniemulsification of the overall mixture solution was achieved by ultrasonicating the mixture for 10 min. The prepared miniemulsion was removed to a three-necked flask (50 mL) fitted with a paddle with Teflon rod and a condenser. After degassed with nitrogen for 30 min, the miniemulsion was heated to 70 °C. The KPS (0.02 g) was added subsequently to initiate the polymerization. The whole synthetic process was kept under mechanical stirring for 8 h in N_2.

2.2.2. Sulfonation of PS nanosheets

PS nanosheets (0.1 g) were dispersed in concentrated sulfuric acid (3 g) at 40 °C for 8 h. After that, the sulfonated polystyrene (SPS) nanosheets were purified by washing with ethanol/water.

2.2.3. Titania composite nanosheets

SPS nanosheets (0.1 g) were dispersed in the mixture of TBT and ethanol (5 mL) (volume ratio = 1) by sonication. After holding the mixture under stirring for 24 h at room temperature, the TBT adsorbed nanosheets were separated by centrifugation and washed with ethanol to remove residual TBT outside the nanosheets. They were then redispersed in the mixture of H_2O and ethanol (5 mL) (volume ratio = 1) under sonication followed by a sol-gel process for 12 h at ambient temperature. The formed composite nanosheets were centrifugated and washed with ethanol/water. To obtain pure inorganic titania nanosheets, the titania composite nanosheets were calcined at 450 °C in air for 4 h.

2.2.4. Silica composite nanosheets

SPS nanosheets (0.1 g), water (1 mL) and TEOS (1 g) were dispersed in ethanol (5 mL) by sonication. After stirring the mixture for 24 h at room temperature, the prepared SPS nanosheets hybridized with silica were purified by centrifugation and washed with ethanol. To obtain pure mesopore inorganic silica nanosheets, the silica composite nanosheets were calcined at 450 °C in air for 4 h.

2.2.5. Ag composite nanosheets

SPS nanosheets (0.1 g) were immersed in aqueous solution of silver nitrate (4 mL) with the concentration of 20 wt.% under stirring for 24 h for absorption. Afterwards the silver nitrate saturated polystyrene nanosheets were separated by centrifugation and further washed with water to remove residual silver ions outside the nanosheets. In a closed vessel, the nanosheets were redispersed in ethanol (4 mL). Then the aqueous solution of sodium borohydride (20 wt.%) was dropped into the dispersion until the color changed under stirring. Subsequently, it was reacted at ambient temperature for 0.5 h leading to Ag composite nanosheets.

2.2.6. Polyaniline (PANi) composite nanosheets

SPS nanosheets (0.1 g) were dispersed in water (5 mL) containing monomeric aniline (0.1 g) by sonication. After degassed with nitrogen for 30 min, the mixture was sealed and stirred for 24 h at ambient temperature. The degassed aqueous ammonium persulfate (1 M, 1 mL) was then added to initiate polymerization of aniline at room temperature for 24 h. The obtained PANi composite nanosheets were purified by centrifugation and washed with water.

2.2.7. Carbon and carbon composites nanosheets

The composite nanosheets were firstly heated to 200 °C at 2 °C/min and held at 200 °C for 2 h, and then were heated to 370 °C. After holding at 370 °C for 2 h, the temperature was further increased to 800 °C and held for 2 h to prepare carbon, silica/carbon and titania/carbon nanosheets. The heated samples were naturally cooled down to ambient temperature. The whole process was conducted under N_2.

2.3. Characterization

Fourier-Transform Infrared (FT-IR) spectroscopy was recorded by a deuterate triglycine sulfate (DTGS) detector on a Bruker EQUINOX 55 spectrometer and processed by the Bruker OPUS program. Raman spectra of the carbon nanosheets were characterized by Renishaw 2000. The samples were prepared by milled with potassium bromide (KBr) to form a very fine powder and then compressed into a thin pellet.

Transmission electron microscopy (TEM) images were obtained using a JEOL 100CX instrument operated at an accelerating voltage of 100 kV. The samples were prepared by spreading very dilute ethanol dispersions onto the carbon-coated copper grids and left to dry.

Scanning electron microscopy (SEM) images were obtained using a HITACHI S-4300 instrument operated at an accelerating voltage of 15 kV. The SEM samples were ambient dried and vacuum sputtered with Pt about an average thickness of 3 nm.

Atomic force microscope (AFM) images were obtained by a Nanoscope IIIA (Digital Instrument) at the tapping mode with silicon tips. The samples were prepared by spin-casting the diluted mother miniemulsion on a clean mica surface at a rotary speed of 500 rpm for 1 min.

Wide-angle X-ray powder scattering (XRD) (Rigaku D/max-2500) was used to characterize the crystalline phase.

Pore size was characterized by nitrogen adsorption/desorption on a Micromeritics ASAP 2020M surface area and porosity analyzer.

3. Results and discussion

3.1. Preparation of curved PS nanosheets

In the O/W miniemulsion polymerization system, the dispersed spherical oil droplets were used as the polymerizing places, which

endowed the formed polymer particles with ideal curved configuration. As a result, if interfacial polymerization was carried out in this O/W miniemulsion system, the spherical hollow polymer particles or the curved nanosheets can be expected in theory.

Here, the used O/W miniemulsion system was comprised of St as monomer, DVB as cross-linker, TD/OT as hydrophobic oil, SDS as surfactant, and KPS as initiator, where the dispersed oil droplets mixed by St, DVB and TD/OT was stabilized by surfactant, SDS, in the continuous water phase, and the initiator, KPS, was dissolved in the water phase. At the beginning of the polymerization, the water soluble radical from KPS initiated the copolymerization of St and DVB at the interface and subsequently the copolymerization of St and DVB carried out in the whole oil droplets. With the polymerization carrying out further, the obtained cross-linked PS oligomer deposited at the interface of oil droplets since PS are soluble neither in water nor in hydrophobic oil. Then this phase-separated polymer served as loci for the further polymerization. In this whole miniemulsion polymerization process, we found that the properties of the hydrophobic oil and usage of the cross-linker were the two vital factors for controlling the morphologies of the obtained polymer nanoobjects.

To study the influence of hydrophobic oil, except for the ratio of TD to OT, the other parameters were kept the same in the whole studied miniemulsion systems, where the cross-linker DVB with a volume ratio of 1:3 to St was used. Fig. 1 was the representative SEM and TEM pictures of the prepared nanoobjects, which clearly showed that the morphologies of nanoobjects could be manipulated only by changing the volume ratio of OT and TD. As shown in Fig. 1A, by using pure OT as hydrophobic oil, the solid particles with the average diameter of ca. 30 nm and a minority of hollow microspheres with the diameter of hundreds of nanometers were formed. By adding a small amount of TD (0.5%, volume ratio) into the hydrophobic oil, the hollow microspheres with clearer void were still obtained but the amount of small solid particles markedly decreased (Fig. 1B). Increasing the volume ratio of TD to 15%, the small solid particles nearly disappeared and small holes appeared on the surface of hollow microspheres at the same time (Fig. 1C). With further increasing the volume ratio of TD to 50%, the size of the holes on the surface of hollow microspheres became increasingly larger and the small solid particles completely vanished (Fig. 1D). When the volume ratio of TD reached 75%, the hollow microspheres were replaced by the novel curved sheet-like

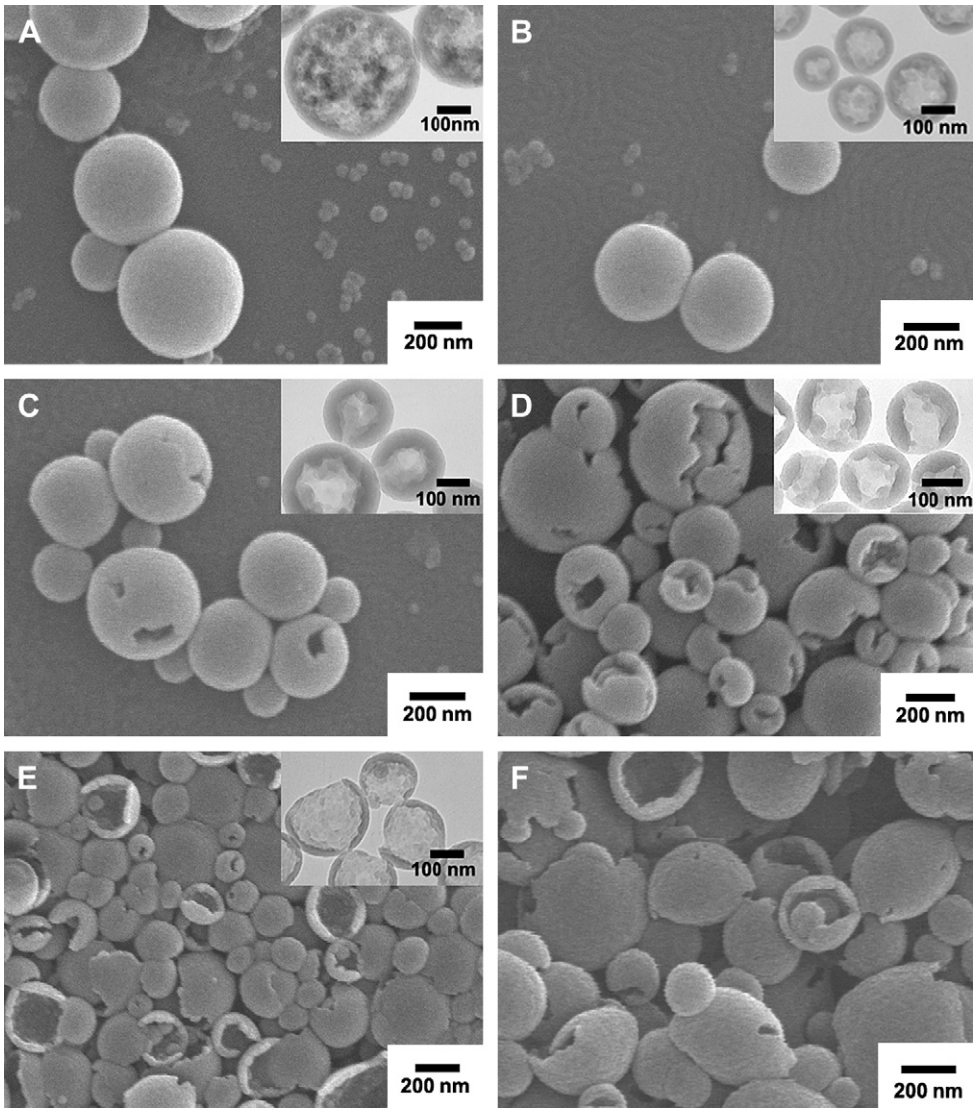

Fig. 1. SEM and inset TEM images of the representative PS hollow microspheres (A–D) and nanosheets (E, F) prepared by miniemulsion polymerization using KPS as initiator, where the TD volume percentages in the mixture of TD and OT were 0% (A), 0.5% (B), 15% (C), 50% (D), 75% (E) and 100% (F), respectively.

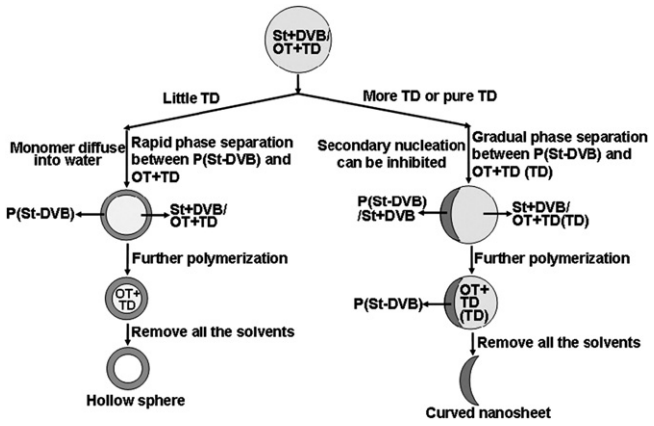

Scheme 1. The proposed mechanism of the formation of PS hollow microspheres and nanosheets by miniemulsion polymerization.

nanoobjects (Fig. 1E). Fig. 1F showed the curved nanosheets obtained by using pure TD as the hydrophobic oil, where the sheet-like appearance was similar to that shown in Fig. 1E.

Furthermore, to show the crucial effect of water soluble initiator, such as KPS, on this method, the corresponding SEM and TEM results with oil soluble AIBN as initiator were also shown in Figure S1. From Figure S1 A to D, comparing to Fig. 1A, C, E, F respectively where all experimental conditions were kept same except for the type of initiator, the solid particles with distinctly different morphologies were obtained by using AIBN as initiator. As a result, it is necessary to use water soluble KPS as initiator for these hollow microspheres and curved nanosheets by our technique here.

It has been reported that the morphology of hollow microspheres prepared by membrane emulsification and subsequent suspension polymerization is caused by a rapid phase separation of formed polymer from the hydrophobic oil cores of the oil droplets [36–38]. When the phase separation process is too slow, the deposited polymer at the interface can not prevent the hydrophobic oil cores from contacting with the continuous water phase during polymerization, which results in the formation of hollow microspheres with pores on their surface.

Scheme 1 showed the formation mechanism of PS hollow spheres and nanosheets in our miniemulsion polymerization system. Because of the shorter alkyl chain length, the solubility between water and OT is better than that between water and TD having longer alkyl chain. As a result, when pure OT was used as hydrophobic oil, St can not be effectively prevented to diffuse from hydrophobic oil droplets to the continuous aqueous phase. Resultantly, the formed PS deposited at the interface from hydrophobic oil right away because of the less St, the good solvent for PS, existing inside the droplets, which resulted in the formation of hollow microspheres. Simultaneously, St diffused into the aqueous phase was also initiated to form small solid particles by a secondary nucleation process. However, TD, having lower solubility in water, can effectively prevent the diffusion of St from the oil droplets. When it was used as hydrophobic oil, the secondary nucleation to get small solid particles was avoided efficiently, because of nearly no escaped St in the aqueous phase. At the same time, the formed polymer can not deposit at the interface quickly from hydrophobic oil because of the high concentration of St, the good solvent of PS, in the oil droplets. Consequently, the curved PS nanosheets were obtained.

As a result, through changing the property of hydrophobic oil simply by adjusting TD/OT with different ratio, the shapes of obtained nanoobjects were easily manipulated. Furthermore, the usage of more hydrophobic oil phase, for example, TD, was critical for the formation of curved PS nanosheets.

On the other hand, for a stable formation of the PS nanosheets, the cross-linked internal structure was also an inevitable factor. Fig. 2 showed the representative SEM and TEM photographs of nanoobjects obtained by using pure St (A) and pure DVB (B) as monomer, respectively, where the hydrophobic oil was all composed by pure TD. By using the pure St as monomer, because of the noncross-linked molecular structure characteristic, the deposited PS single chain at the interface can easily change their location to maintain a minimum surface energy when TD moved to contact with aqueous phase during the whole miniemulsion polymerization. After the miniemulsion polymerization was finished, the disk-like nanoobjects with smooth face were obtained (Fig. 2A). However, when the DVB was used as sole monomer, the polymer deposited at the interface having a cross-linked structure. With the hydrophobic oil moving to contact with the aqueous phase during the polymerization, the cross-linked internal structure locked the polymer chain and kept the original rough curved sheet-like morphology. As a result, after the polymerization was finished, the curved nanosheets with rough internal surface were obtained (Fig. 2B).

It was also reported that the high vacuum required for SEM sample preparation and measurement may cause the integrated microspheres with indentations on their surface sometimes [39]. To exclude this possibility of producing curved nanosheets, except for SEM and TEM, AFM was also used to observe the morphology of the obtained nanoobjects before (Fig. 3A) and after (Fig. 3B) high vacuum disposal which was kept the same as that performed in SEM. Compared Fig. 3A with Fig. 3B, there was no difference in the appearance between them. Accordingly, we concluded that the

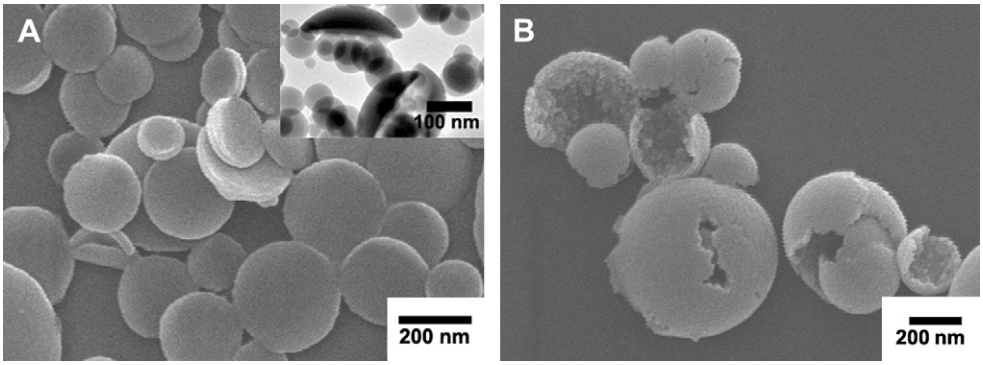

Fig. 2. SEM and inset TEM images of the nanosheets prepared by miniemulsion polymerization with TD as hydrophobic oil. The St (A) and DVB (B) was homopolymerized, respectively.

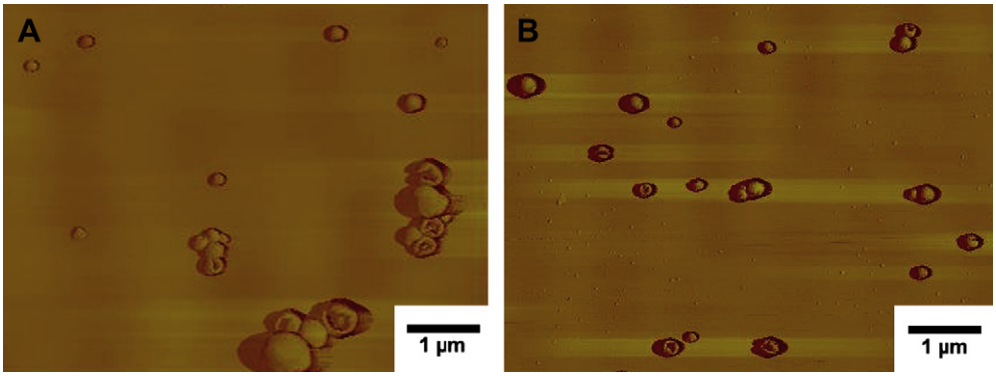

Fig. 3. AFM images of the obtained PS nanosheets before (A) and after (B) dealing with high vacuum respectively.

novel curved sheet-like nanoobjects were brought by the property of the used miniemulsion polymerization itself.

As a result, by simply choosing TD with longer alkyl chain as hydrophobic oil and using the cross-linker of DVB, we successfully prepared stable PS nanosheets with a novel curved morphology by miniemulsion polymerization.

3.2. Preparation of curved composite nanosheets with controlled compositions and porous nanosheets thereof

Using the PS hollow microspheres as templates, a series of composite hollow microspheres with changeable compositions and controlled microstructure were obtained in our group in recent years [40–43]. Here, we extended the same concept to prepare another kind of novel curved sheet-like organic/inorganic nanocomposites with various compositions, by using the formed curved PS nanosheets as templates. Furthermore, based on the obtained curved sheet-like inorganic/organic nanocomposites, we also prepared porous curved sheet-like inorganic nanomaterials.

3.2.1. Sulfonated PS nanosheets and carbon nanosheets thereof

To prepare the SPS nanosheet gel, the obtained curved PS nanosheets with cross-linked internal structure were treated by concentrated sulfuric acid at the temperature of 40 °C for 8h. After this process, the curved sheet-like morphology was still preserved well, which was proved by SEM picture shown in Fig. 4A. FT-IR spectrum was used to track the reaction of sulfonation. As shown in Figure S2A, the characteristic bands at 670, 1180 and 1222 cm^{-1} were assigned to the derived sulfonic acid group ($-SO_3H$) and the band at 1128 cm^{-1} was related with the sulfone group ($-SO_2-$). Furthermore, using the SPS nanosheets as templates, porous carbon nanosheets were prepared through carbonization process at high temperature of 800 °C. Fig. 4B showed the SEM image of the resulted carbon nanosheets, which still preserved their original curved sheet-like formation. Raman (Figure S3A) and XRD (Figure S3B) results indicated that the phase of obtained carbon was amorphous. The nitrogen adsorption/desorption isotherms (Trace I, Fig. 5) indicated the presence of mesopores and micropores in the shell of the obtained carbon nanosheets. The BET specific surface area was 550.19 $m^2\ g^{-1}$ and t-plot specific surface area contributed by the micropore was 470.92 $m^2\ g^{-1}$. The total pore volume was 0.31 $cm^3\ g^{-1}$, to which the micropore contributed 0.23 $cm^3\ g^{-1}$. The micropore diameter was around 0.45 nm and the mesopore size was around 40 nm.

3.2.2. Titania composite nanosheets

Inorganic/organic semiconductor titania composite nanosheets were prepared by favorable sol–gel process of TBT within the SPS nanosheets. Fig. 4C showed the resulted titania inorganic/organic composite nanosheets with a similar morphology to that of their templates (Fig. 4A). Figure S4A showed the XRD curve of the formed titania in this state, where its phase was amorphous. The prepared titania composite nanosheets were strong enough to survive calcination at 450 °C in air, which removed the polymer composition (Fig. 4D). Furthermore, carbonizing the sheet-like titania/SPS nanocomposites also converted them into titania/carbon composite nanosheets (Fig. 4E). As shown in Fig. 4D and E, compared with Fig. 4A, a significant volume contraction of the obtained nanosheets was observed because of calcination and carbonization process but the curved sheet-like morphology still remained clearly. Besides, the calcination and carbonization process also caused the phase transformation of titania inorganic composition from amorphous to anatase or rutile, which was verified by XRD (Figure S4). XRD results shown in Figure S4B proved that the calcined titania was composed of anatase (Figure S4B) and a higher carbonization temperature (800 °C) resulted in a dominant rutile phase with a small amount of the anatase phase (Figure S4C).

3.2.3. Silica composite nanosheets

When using SPS nanosheets as templates and TEOS as sol–gel agent, silica/SPS inorganic/organic composite nanosheets were also prepared by a simple sol-gel process, where the sulfonic acid group of SPS catalyzed the hydrolysis and condensation reactions of TEOS. Shown in Fig. 4F was the corresponding SEM image of the obtained silica/SPS composite nanosheets, where the curved sheet-like morphology was still clear and similar with their templates shown in Fig. 4A. Subsequently, removing the organic SPS composition of the silica/SPS composite nanosheets by calcination process at 450 °C under air could prepare porous inorganic silica nanosheets. Fig. 4G was the SEM image of the obtained silica nanosheets. Compared with Fig. 4A, the curved sheet-like formation was still preserved well, which meant that the formed inorganic silica composition in silica/SPS nanocomposites having a continuous structure. Shown in Fig. 5 (Trance Π) was the corresponding nitrogen adsorption/desorption isotherms of inorganic silica nanosheets, from which the BET specific surface area was calculated to be 424.75 $m^2\ g^{-1}$ and the t-plot micropore surface area was as small as 42.47 $m^2\ g^{-1}$. Otherwise, the silica/carbon composite nanosheets were also prepared by carbonizing the silica/SPS nanocomposites at the high temperature of 800 °C under nitrogen. Fig. 4H showed the representative SEM image of the silica/carbon composite nanosheets, whose morphology was similar to that shown in Fig. 4F and G. Fig. 5 (Trance Ш) was the corresponding nitrogen adsorption/desorption isotherms of silica/carbon composite nanosheets, where the BET specific surface area was 552.84 $m^2\ g^{-1}$ and the t-plot micropore surface area was

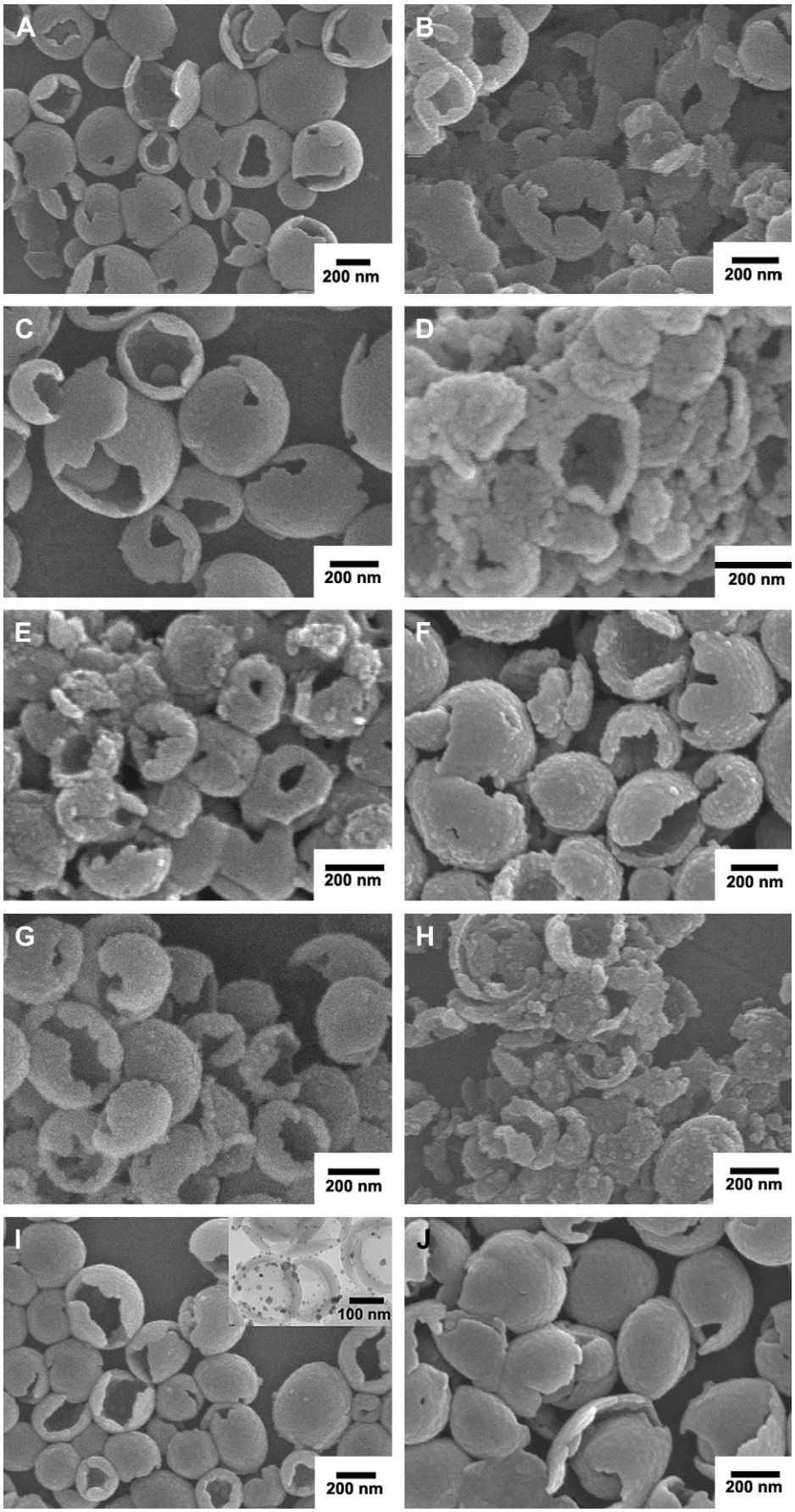

Fig. 4. SEM and inset TEM images of the representative functional nanosheets. SPS nanosheets (A) and the corresponding carbon nanosheets (B), tiatnia/SPS composite nanosheets (C) and the derived inorganic tiatnia (D) and titania/carbon (E) nanosheets, silica/SPS composite nanosheets (F) and the derived inorganic silica (G) and silica/carbon (H) nanosheets, Ag nanoparticles/SPS composite nanosheets (I), PANi/SPS composite nanosheets (J).

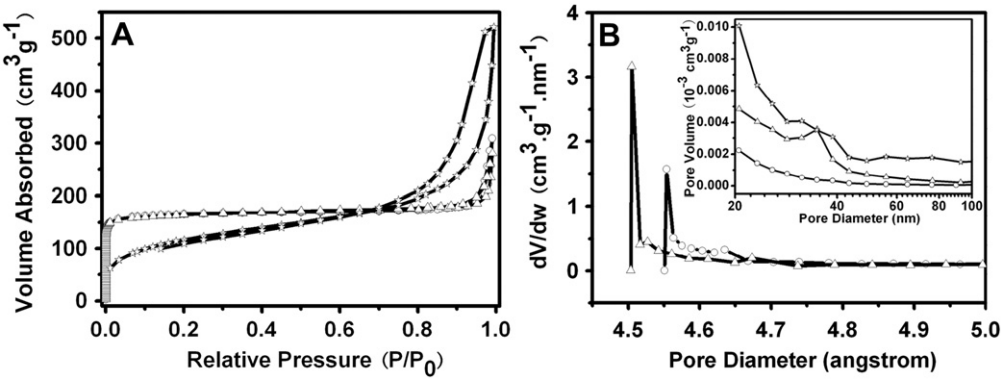

Fig. 5. Nitrogen adsorption/desorption isotherms of the carbon nanosheets, silica nanosheets and carbon composite nanosheets (A), and the corresponding pore size distribution (B). △ (I): carbon nanosheets derived from SPS gel nanosheets; ☆ (II): the silica nanosheets after removal of PS by calcination at 450 °C in air from the silica/PS composite nanosheets; ○ (III): silica/carbon composite nanosheets after carbonizing the silica/SPS nanocomposites at the high temperature of 800 °C under nitrogen.

485.39 m^2 g^{-1}. As a result, the resulted silica/carbon composite nanosheets had two pores with different diameter, the micropores and the mesopores with mean diameter of 0.46 nm and 22 nm, respectively.

3.2.4. Ag composite nanosheets

The negatively charged sulfonated gel layer can also be used to adsorb metal cations. After a reduction reaction of the adsorbed metal cations in the SPS nanosheets, other kinds of curved inorganic/organic composite nanosheets with metal nanoparticles could be obtained. Here, we chose preparation of Ag/SPS composite nanosheets to demonstrate this concept. Fig. 4I was the representative SEM and TEM (inset) images of the obtain Ag/SPS composite nanosheets, which showed that the Ag nanoparticles with a mean diameter of 10 nm were formed and well distributed in the whole curved shell of SPS nanosheets. The cubic phase of the synthesized silver nanoparticles was also confirmed by XRD as shown in Figure S5, where all of the four broad peaks at 38.21, 44.31, 64.61 and 77.71 were similar to the standard (JCPDS card file no. 4_783+) and the broader part in the low scan angle could be attributed to the amorphous polymer PS.

3.2.5. PANi composite nanosheets

Aniline monomer can also be perfectly adsorbed within the shell of SPS gel by specific interaction. As a result, the PANi/SPS composite nanosheets were prepared after in-situ polymerization of the adsorbed aniline monomer. Fig. 4J showed the representative SEM image of the curved sheet-like PANi/SPS nanocomposite, where their morphology were similar to their templates shown in Fig. 4A. The FT-IR spectrum of the PANi/SPS composite nanosheets was shown in Figure S2B, where the PANi in situ doped by the sulfonic acid (in the gel shell) in the form of emeraldine salt was evidenced. The main peaks at 1583 and 1498 cm^{-1} corresponded to stretching deformations of quinone and benzene rings, respectively. The bands at 1303, 1157 and 843 cm^{-1} could be assigned to C–N stretch in a secondary aromatic amine, the aromatic C–H in plane bending modes, and the out of plane deformations of C–H in the 1,4-disubstituted benzene ring, respectively. The bands at 1303, 1157, and 843 cm^{-1} were identical to the emeraldine salt form of PANi [44,45]. The conductivity of the PANi/SPS composite nanosheets was 7.2×10^{-4} S/cm.

4. Conclusions

We have reported a novel no-template method to prepare PS nanosheets with curved morphology and stable cross-linked internal structure by one-pot miniemulsion polymerization. The successful secrets of this method lie in two aspects. One is that the used oil phase must have high hydrophobicity and also must be a good precipitator for the formed PS, which guaranteed that the polymerization loci were confined at the interface between oil droplets and water in the miniemulsion system to obtain the curved sheet-like morphology. The other is the use of the cross-linking comonomer, which gives a cross-linked internal structure within the shell of nanosheets to protect the original curved sheet-like morphology from damaging by the movement of PS chains during the whole polymerization process. Based on the same polymerization concept, we think this simple and effective method for preparing curved nanosheets can be expanded to many other different kinds of polymers theoretically. Furthermore, we also show that these curved PS nanosheets can also be used as a general template to prepare curved sheet-like nanocomposites with various kinds of compositions such as metals, inorganic oxides and even organic functional polymers. As a result, a novel family of composite nanomaterials with curved sheet-like morphology and controllable functionalities is expected.

Acknowledgements

We thank financial support by the NSF of China (50373004, 50733004, 20720102041 and 20128004), Chinese Academy of Sciences, China Ministry of Science and Technology (KJCX2-YW-H20 and 2006CB605300), Beijing Municipal Commission of Education and the Scientific Research Foundation of Beijing Normal University (2009SC-1).

Appendix A. Supplementary material

Supplementary data associated with this article can be found, in the online version, at doi:10.1016/j.polymer.2010.04.056

References

[1] Xia YN, Yang PD, Sun YG, Wu YY, Mayers B, Gates B, et al. Adv Mater 2003;15:353–9.
[2] Sasaki T, Watanabe M. J Phys Chem B 1997;101:10159–61.
[3] Sasaki T, Ebina Y, Kitami Y, Watanabe M. J Phys Chem B 2001;105:6116–21.
[4] Kleinfeld ER, Ferguson GS. Science 1994;265:370–3.
[5] Kotov NA, Haraszti T, Turi L, Zavala G, Geer RE, Dékány I, et al. J Am Chem Soc 1997;119:6821–32.
[6] Nakano H, Ishii M, Nakamura H. Chem Commun 2005;23:2945–7.
[7] Sasaki T, Watanabe M. J Am Chem Soc 1998;120:4682–9.
[8] Lee JH, Shin DW, Makotchenko VG, Nazarov AS, Fedorov VE, Kim YH, et al. Adv Mater 2009;21:4383–437.
[9] Kim JU, Cha SH, Shin K, Jho JY, Lee JC. Adv Mater 2004;16:459–64.
[10] Wang JJ, Zhu MY, Outlaw RA, Zhao X, Manos DM, Holloway BC. Carbon 2004;42:2867–72.

[11] Wang WW, Zhu YJ, Cheng GF, Huang YH. Mater Lett 2006;60:609–12.
[12] Dai ZR, Pan ZW, Wang ZL. J Phys Chem B 2002;106:902–4.
[13] Vadivel Murugan A, Muraliganth T, Manthiram A. Chem Mater 2009;21:5004–6.
[14] Hu LH, Peng Q, Li YD. J Am Chem Soc 2008;130:16136–7.
[15] Wu BH, Guo CY, Zheng NF, Xie ZX, Stucky GD. J Am Chem Soc 2008;130:17563–7.
[16] Sathish M, Miyazawa K. J Am Chem Soc 2007;129:13816–7.
[17] Matsui J, Mitsuishi M, Aoki A, Miyashita T. J Am Chem Soc 2004;126:3708–9.
[18] Groenewolt M, Thomas A, Antonietti M. Macromolecules 2004;37:4360–4.
[19] Kawano S, Nishi S, Umezaa R, Kunitake M. Chem Commun; 2009:1688–90.
[20] Okubo M, Izumi J, Takekoh R. Colloid Polym Sci 1999;277:875–80.
[21] Han SH, Ma JH, Du YZ, Omi S, Gu LX. J Appl Polym Sci 2003;90:3811–21.
[22] Okubo M, Takekoh R, Izumi J. Colloid Polym Sci 2001;279:513–8.
[23] Okubo M, Yamaguchi A, Fujiwara T. Colloid Polym Sci 1999;277:1005–8.
[24] Mock EB, Bruyn HD, Hawkett BS, Gilbert RG, Zukoski CF. Langmuir 2006;22:4037–43.
[25] McDonald CJ, Devon MJ. Adv Colloid Interface Sci 2002;99:181–213.
[26] Landfester K. Angew Chem Int Ed 2009;48:4488–507.
[27] Landfester K. Adv Mater 2001;13:765–8.
[28] Nelliappan V, El-Aasser MS, Klein A, Daniels ES, Robers JE. J Polym Sci Part A Polym Chem 1996;34:3173–81.
[29] Landfester K, Antonietti M. Macromol Rapid Commun 2000;21:820–4.
[30] Lu W, Chen M, Wu LM. J Colloid Interface Sci 2008;328:98–102.
[31] Colver PJ, Colard CAL, Bon SAF. J Am Chem Soc 2008;130:16850–1.
[32] Tiarks F, Landfester K, Antonietti M. Langmuir 2001;17:908–18.
[33] Matyjaszewski K. Biomacromolecules 2009;10:2300–9.
[34] Chen J, Zeng F, Wu SZ, Su JH, Tong Z. Small 2009;5:970–8.
[35] Koh HD, Changez M, Lee JP, Lee JS. Macromol Rapid Commun 2009;30:1583–8.
[36] Ma GH. Macromol Symp 2002;179:223–40.
[37] Ma GH, Omi S, Dimonie VL, Sudol ED, EL-Aasser MS. J Appl Polym Sci 2002;85:1530–43.
[38] Ma GH, Chen AY, Su ZG, Omi S. J Appl Polym Sci 2003;87:244–51.
[39] Esen C, Kaiser T, Borchers MA, Schweiger G. Colloid Polym Sci 1997;275:131–7.
[40] Niu ZW, Yang ZZ, Hu ZB, Lu YF, Han CC. Adv Funct Mater 2003;13:949–54.
[41] Yang ZZ, Niu ZW, Lu YF, Hu ZB, Han CC. Angew Chem Int Ed 2003;42:1943–5.
[42] Yang M, Ma J, Zhang CL, Lu YF, Yang ZZ. Angew Chem Int Ed 2005;44:6727–30.
[43] Ding SJ, Zhang CL, Yang M, Qu XZ, Lu YF, Yang ZZ. Polymer 2006;47:8360–6.
[44] Zeng XR, Ko TM. J Polym Sci Part B Polym Phys 1997;35:1993–2001.
[45] Quillard S, Louam G, Buisson JP, Boyer M, Lapkowski M, Pron A, et al. Synth Met 1997;84:805–6.